Turkish Journal of Earth Sciences (Turkish J. Earth Sci.), Vol. 19, 2010, pp. 513–526. Copyright ©TÜBİTAK
doi:10.3906/yer-0903-2 First published online 17 November 2009

Application of the Normalized Full Gradient (NFG) Method to Resistivity Data

ALİ AYDIN

Department of Geophysical Engineering, Pamukkale University, TR–20020 Denizli, Turkey
(E-mail: aaydin@pau.edu.tr)

Received 10 March 2009; revised typescript receipt 08 June 2009; accepted 17 November 2009

Abstract: This paper proposes the application of the normalized full gradient (NFG) method to resistivity studies and illustrates that the method can greatly reduce the time and work load needed in detecting buried bodies using resistivity measurement. The NFG method calculates resistivity values at desired electrode offsets by extrapolation of a function of resistivity measurements (i.e. the gradient) to other depth levels using resistivity measurements done at one electrode offset only. The performance and reliability of the NFG method is tested on laboratory and field resistivity data from two sites by comparing the trend of the resistivity values at six or more electrode offsets, with the trend calculated at the same electrode offsets using the NFG method. The first area is in Rize (NE Turkey) where a resistivity survey was conducted to locate a metal tailings pipeline in unconsolidated gravel deposited by a nearby stream. The second field site is in Trabzon (NE Turkey), where the purpose of the resistivity survey was to map the boundaries of a landslide in clay, marl and geologic units.

Key Words: Normalized Full Gradient, resistivity modelling, Çayeli, Gürbulak

Normalize Edilmiş Tam Gradyan Yönteminin Özdirenç Verisine Uygulanması

Özet: Bu makale Normalize Edilmiş Tam Gradyan (NTG) yönteminin özdirenç çalışmalarında kullanımını ve aynı zamanda da bu yöntemin gömülü cisimlerin belirlenmesinde özdirenç ölçülerine zaman ve iş yönüyle büyük kolaylık sağladığını işlemektedir. NTG yöntemi, bir elektrot açılımındaki özdirenç ölçüleri kullanılarak, diğer derinlikler için özdirenç ölçülerinin bir fonksiyonuna yaklaşımıyla (gradyanı) istenen elektrot açıklığında gerçek özdirenç değerlerinin hesaplanmasına yardımcı olmaktadır. NTG yöntemi basit model yapılarına ve farklı problemlere sahip iki saha çalışmasına uygulandı. Bunlardan birincisi çakıl taşı yığını içinde yer alan metal artık borusunun uzanımının arandığı Rize'nin doğusunda (KD Türkiye) yapılan, diğeri ise kil, marn ve kumtaşı jeolojik birimleri içinde yer alan heyelanın kayma sınırları göstermek için Trabzon'nun (KD Türkiye) güneyinde yapılan bir çalışmadan alınmıştır. Basit modellerde ve saha özdirenç kaynaklarının oldukça duyarlı tanımlanmasında, NTG yönteminin çok doğru çalıştığı gösterilmiştir.

Anahtar Sözcükler: Normalize Edilmiş Tam Gradyan, özdirenç modelleme, Çayeli, Gürbulak

Introduction

Resistivity measurements in the field are done by a series of measurements on the surface of the earth by what is called a spread for each depth level, done by altering the electrode spacing in accordance with the depth level, with larger electrode spacing imaging deeper layers. The time of the resistivity measurements is proportional to the number of depth levels needed to be measured. This is particularly true in field situations where only a 4-electrode system is deployed for the resistivity surveys.

The method proposed in this paper reduces the total number of depth levels to be measured to exactly one, reducing the cost by a factor that is equal to the depth levels needed. This method, the normalized full gradient (NFG) method, is one of the most successful procedures used in the determination of singular points of the potential fields (Sındırgı *et al.* 2008).

The use of NFG method in geophysics is not new. Indeed, it has been successfully used for about a half century in exploration for hydrocarbon reserves. The method was first used by Strakhov (1962) and Golizdra (1962), who were followed by other researchers in the former Soviet Union (e.g., Berezkin & Buketov 1965; Berezkin 1973; Mudretsova *et al.* 1979; Berezkin & Filatov 1992). The method was used more frequently during and after the 1990s (e.g., Lyatsky *et al.* 1992; Aydın 1997, 2007; Pašteka 2000; Aydın *et al.* 2002; Eliseeva *et al.* 2002; Ebrahimzadeh 2004). There are also papers on the application of the NFG method to gravity and magnetic studies (e.g., Aydın *et al.* 1997; Aydın 2000). This method was also used for interpreting self potential (Sındırgı *et al.* 2008), seismic (Karslı 2001), and electromagnetic data (Dondurur 2005). A good description of the use of the NFG method in the interpretation of airborne electromagnetic and magnetic data was given by Traynin & Zhdanov (1995). Sındırgı *et al.* (2008) successfully used the NFG method and demonstrated that it worked perfectly when the structure model was simple. They concluded that natural potential sources close to earth's surface were identified by the method more accurately at greater harmonics, while deep sources were identified at lesser harmonics. Because Sındırgı *et al.* (2008) applied the NFG method to theoretical data from simple sphere, cylinder and vertical sheet models, in this study NFG is not applied to these simple models.

Here, the NFG method is introduced as an alternative to electrical resistivity interpretation tools: an application which has apparently never been developed before. In this paper, the NFG method is first briefly explained and then its application to one laboratory and two field resistivity surveys will be illustrated, providing evidence that it is a new and more robust approach to the interpretation of resistivity data.

The Normalized Full Gradient (NFG) Method

The main purpose of the NFG method in the interpretation of potential fields is data extrapolation using some functions that are analytical everywhere except where the sources are. If such functions exist and a measurement at one depth level is available, then these functions can be extrapolated downward (or upward, to be more exact) to predict some shape or distribution of the source locations at other depth levels. The method is especially useful in detecting characteristic points of such structures as centres and corners from singular points in the potential fields.

Berezkin (1973) described such a function that was obtained from the horizontal and vertical gradients of the observed potential data. The existence of such a function was shown by Strakhov *et al.* (1977). Traynin & Zhdanov (1995) used such functions to interpret electromagnetic data. Here, the theory behind the method is briefly summarized.

Let W(x, z) represent an analytical function of two variables, x (horizontal position) and z (vertical position). Then the Fourier transform, F (k), of its horizontal derivative

$$F(k) = FT\left[\frac{\partial W}{\partial x}\right] \tag{1}$$

relates to the Fourier transform, H (k), of the vertical derivative,

$$H(k) = FT\left[\frac{\partial W}{\partial z}\right] \tag{2}$$

by:

$$H(k) = i\,\mathrm{sgn}(k)F(k) \tag{3}$$

where sgn is signum function and $i=(-1)^{1/2}$. Therefore, it follows that (Nabighian 1974) both lateral and vertical derivatives can be expanded into Fourier series in x while containing an exponential term in z. Such an expansion can be found in Bracewell (1984).

For functions that are initially zero and end measurement points (say at x= 0 and x= L) sine only expansion can be used (Rikitake *et al.* 1976)

$$W(x,z) = \sum_{n=0}^{N-1} B_n \sin(k_n x) e^{k_n z} \quad (4)$$

where

$$k_n = \frac{\pi n}{(N-1)\triangle x} \quad (5)$$

represents the discrete wave-numbers (harmonics) and N is the number of the measurements taken along x-axis, and Δx is the distance between them. Fourier coefficients needed for this expansion can be calculated from measurements made at z= 0:

$$B_n = \frac{2}{L}\int_0^L W(x,0)\sin(k_n x)\,dx \quad (6)$$

Then, components of the gradient vector can be calculated as

$$\frac{\partial W}{\partial x} = \frac{\pi}{L}\sum_{n=0}^{N-1} nB_n \cos(k_n x) e^{k_n z} \quad (7)$$

and

$$\frac{\partial W}{\partial z} = \frac{\pi}{L}\sum_{n=0}^{N-1} nB_n \sin(k_n x) e^{k_n z} \quad (8)$$

The magnitude of the gradient vector,

$$G(x_i,z) = \sqrt{\left(\frac{\partial W}{\partial x}\right)^2_{x_i,z} + \left(\frac{\partial W}{\partial z}\right)^2_{x_i,z}} \quad (9)$$

at the measurement points, i= 1,2,.., N, is then calculated and the result is normalized by dividing the result with the average of the gradient vector along space samples, x_i,

$$< G(x,z) > = \frac{1}{N}\sum_{i-0}^{N-1} G(x_i,z) \quad (10)$$

Therefore the normalized full gradient (NFG) is

$$G_n(x_i,z) = \frac{G(x_i,z)}{< G(x,z) >} \quad (11)$$

The bottom line is that the NFG operator can then be calculated at any depth level using Fourier coefficients, B_n, obtained from the measurement of potential W(x,z) at one depth level only, W(x,0). Such a downward continuation process using wave-number domain was also described by Jung (1961).

Improvements of the NFG Function

There are practical issues in using the NFG method described above. The application of the method is as follows. Firstly, the method amplifies high wave-numbers as depth increases which may enhance noise. Secondly, observational errors in the potential measurement at zero depth level, W(x,0), the finiteness of the measurement range L, the interval and Δx, of the measurements all affect the accuracy of the NFG calculations. To compensate for such undesirable effects, it is necessary to suppress high wave-numbers. This is achieved by multiplying the terms in the sum by a function that suppresses high wave-numbers (Berezkin 1988);

$$q_n = \left(\frac{\sin\left(\frac{\pi n}{N}\right)}{\frac{\pi n}{N}}\right)^{\mu} \quad \mu > 0 \quad (12)$$

This term is known as Lancsoz smoothing term, or as the q factor. It modifies the characteristics of the NFG operator. The vertical and horizontal terms are then calculated as

$$\frac{\partial W}{\partial x} = \frac{\pi}{L}\sum_{n=0}^{N-1} nB_n \cos(k_n x) e^{k_n z} q_n \quad (13)$$

and

$$\frac{\partial W}{\partial z} = \frac{\pi}{L}\sum_{n=0}^{N-1} nB_n \sin(k_n x) e^{k_n z} q_n \quad (14)$$

instead of using original expressions given earlier. The behaviour of the q-function as a function of wave-number index, *n*, and damping parameter, μ is shown in Figure 1. Aydın (1997), Karslı (2001), and Dondurur (2005) suggested μ= 1or μ= 2 for reasonable results in downward continuation and μ= 2 is used throughout this study. The q factor, when combined with the factor:

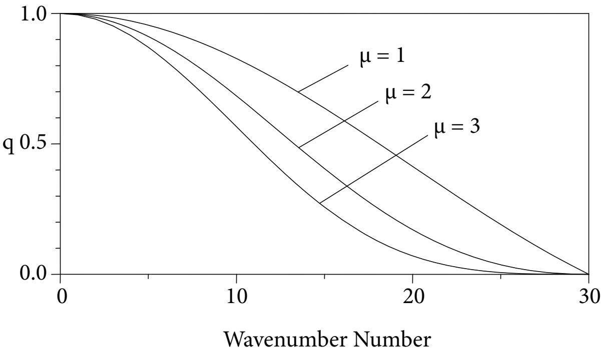

Figure 1. Behaviour of q function.

$$ne^{k_n z} \tag{15}$$

in the series expansion given above, acts like a new function

$$H(n) = ne^{k_n z} q_n \tag{16}$$

which is known as the linear frequency characteristic of the NFG function. This function, also studied in Aydın (2007), shows an increasing damping effect due to the terms *n* as well as q. The function also limits the required number of wave-numbers in the series expansion. Indeed the use of a limited wave-number index range, $[N_1, N_2]$, is common and determined by trial and error. The indices are cut-off points that band limit the function, as used by Berezkin (1988), Aydın (1997) and Dondurur (2005). N_1 is generally selected to be 1 in potential fields and the determination of the harmonic limit was previously discussed methodically by Dondurur (2005). There are issues resulting from the way the integrals are taken in the calculation of Fourier coefficients, B_n, given above. Obviously these integrals can be calculated in many different ways, including the trapezoid method, for discrete data. I use the Filon (1928) method (see also Davis & Robinowitz 1989) as detailed by Aydın (1997). Finally, in order to obtain reliable resistivity interpretations with the NFG method, the profile length needs to be 8 to 10 times the extent of the desired depth section, the measurement interval needs to be at most one tenth of the profile length, measurement precision must be at least 1 Ohm-m, measurement profile needs to be on a line, and the effects of the topography need to be eliminated. These restrictions were defined by Berezkin (1988), Aydın (1997) and Dondurur (2005).

Applications

Synthetic Data

The model resistivities used in the simulations were obtained from a previous study by Kazancı (1997) that was carried out in experimental tanks for conductive and non-conductive structures with simple geometries. The model tank at the Department of Geophysics of Karadeniz Technical University was made up of 8-mm-thick glass and measured 88×90×50cm. The tank was filled with water which was considered as a homogeneous medium around the structure. Thirty-three non-corrosive steel electrodes, each having a diameter of 0.31 cm, were used. The electrodes, 2.54 cm long, were placed in a polyvinyl chloride PVC) stick 83 cm long and 2.4 cm wide. An adjustable power source provided current to the tank. Input current was measured with a Universal Avometer, and the potential values were measured with a digital voltmeter of Kingdom-400 type. A dipole-dipole array was used for the two models that were studied. Apparent resistivity calculations at 6 electrode offsets in the vertical direction and a total of 85 points, in the horizontal direction, were taken for the models having depths of about 7.6 cm.

Apparent resistivity sections were created for the conductive dyke models using a dipole-dipole array (Figures 2h & 3h). The conductive body is a rectangular prism 2×7×0.5 cm of pure aluminium. Resistivity of the medium is 2.67×10^{-8}ohm-m. Depth of the dykes from the water surface is 0.5 cm. The results of resistivity sections are shown on Figure 2a and 3a for the models used in the tank. The position of the body used in these measurements is shown in Figure 2h and 3h respectively. For the vertical dyke, the resistivity values were low over the dyke, and symmetrical anomalies were observed. Computed apparent resistivity values measured range from 10–34 ohm-m. A minimum enclosure occurs at the upper part of the 45° inclined dyke model resistivity section, where the resistivity values range from 100–600 ohm-m, and these minimum values extend along the dyke inclination.

Six NFG sections obtained over the vertical dyke model (using six different wave-number ranges) using the data values recorded at the n= 6 depth level

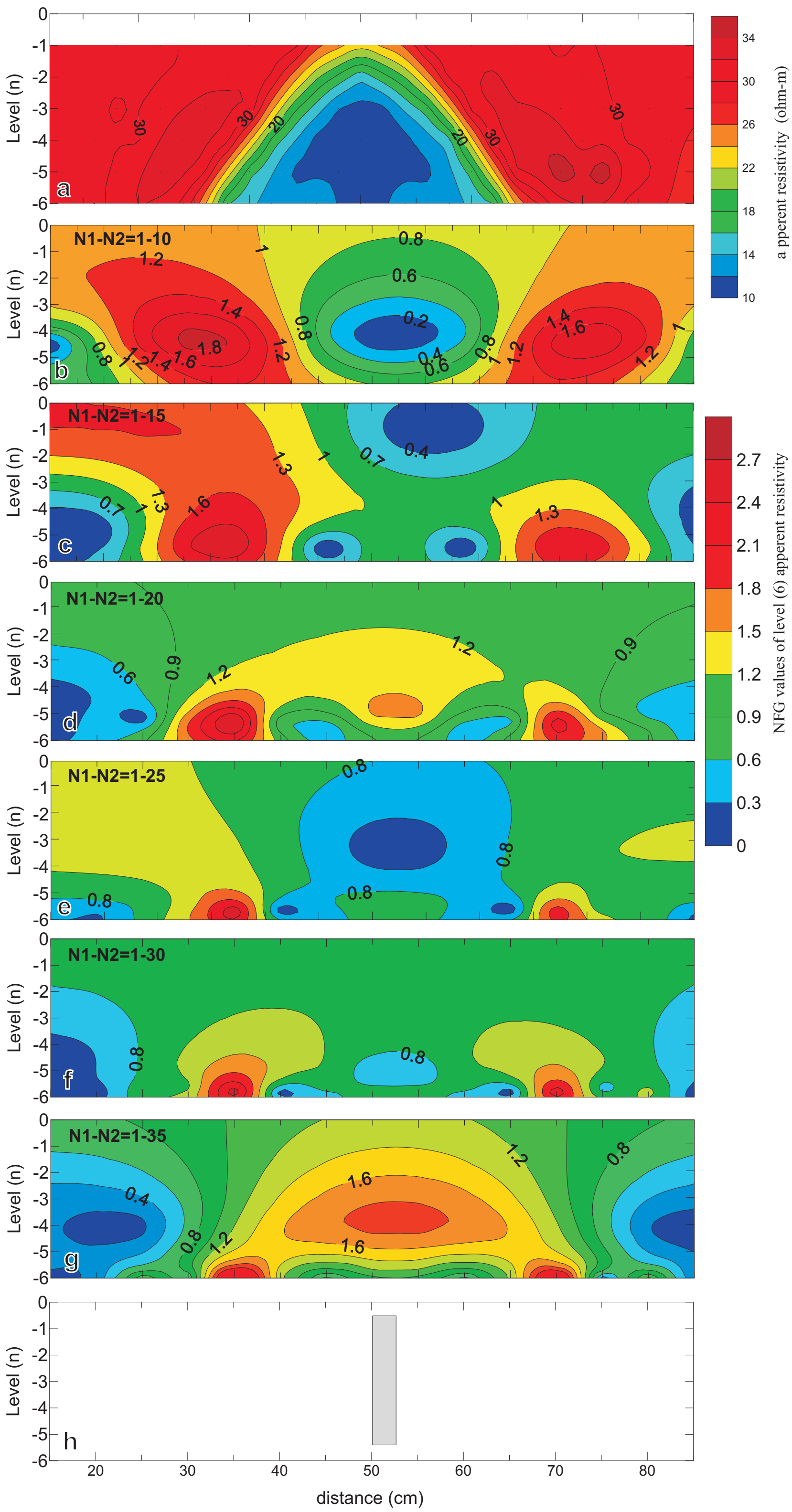

Figure 2. **(a)** Resistivity measurements on vertical dyke (Kazancı 1997), **(b–h)** NFG results, **(i)** the model.

are given in Figure 2b–g. Corresponding figures for the inclined dyke are given in Figure 3b–g. Note that although the effects of the conductive dyke are observed at all the wave-numbers on the NFG sections shown by the vertical dyke model, the most effective responses are observed at ranges [1,10], [1,15], [1,25] and [1,30] for the model. While harmonic resistivity, which is [1,20] and [1,35] respectively, decreases in Figures 2d and 2f, the resistivity increases in Figures 2a and 2b. This variation comes from sixth level data that was extended due to missing data at the end of the profile. So, the NFG section was affected by values at high harmonic sequences. The NFG operator is gradient function so it never gets negative values and values range from 0 to 2, as shown in Figure 2. Values less than 1 are called minimum; otherwise they are called maximum. So, NFG sections never refer to conductor or resistor but give boundaries between resistor and conductor bodies and their depths. It is clear that the position of the anomalous resistivity trend resulting from the dyke in the NFG sections fits the trend of the apparent resistivity distributions obtained from the laboratory measurements (Figure 2a versus 2b and Figure 3a versus 3b). The results obtained with the vertical model (Figure 2b) show the horizontal symmetry expected and present in the apparent resistivity calculations (Figure 2a). In the dipping dyke model, the closure present in the apparent resistivity model (Figure 3a) is also present at the same position in the NFG sections due to unaffected changing shapes of anomalies with different wave-number intervals (Figure 3b–g).

Although determining the range required to achieve stable results is very important, all previous studies showed that N2, the second harmonic, is the most suitable value for ranging between 20 and 30. In fact, the large range of wave-numbers shows that the simulation result of the study is comparable, as demonstrated in Figure 3b–g. However, it did not give the expected result in Figure 2b–g. This part of the NFG method should develop new rules for the use of this method in future work. Rules of thumb regarding dipole-dipole survey line length and spacing are similar to the rules purposed by Berezkin (1988), Aydın (1997) and Dondurur (2005) for gravity, magnetic and electromagnetic data.

Field Surveys

The NFG method was applied to the apparent resistivity sections from two different field sites. The first site is east of Rize (NE Turkey) and apparent resistivity data were acquired to locate a metal tailings pipeline (Figure 4). The measurements were acquired by our working group in 1994. The second field site is located south of Trabzon (NE Turkey) and apparent resistivity data were acquired to delineate the boundaries of a landslide (Figure 7).

Site #1

The first area is around Çayeli, about 20 km east of Rize along the Black Sea coast. The resistivity survey was used to locate a metal tailings pipeline of the Çayeli Cupper Mining Corporation (ÇBİ) as part of a road construction project (Figure 4). The metal tailings pipeline starts about 2 km inland and extends to a mixing tank on the coast. After mixing the tailings with seawater in the tank, the waste is discharged by a pipeline to the seafloor at 350 m depth. The construction of a road along the Black Sea coast required the location of the exact position of the pipeline to be known, since its precise position was previously unknown. Vertical Electrical Soundings (VES) and two 2-dimensional resistivity profiles were acquired in order to determine the horizontal and vertical resistivity distributions in the subsurface. The lengths of these profiles varied between 19 m and 21 m. In general profiles were oriented NW–SE. Since the diameter of the pipeline (50 cm), was very small compared to its depth, in order to get high resolution resistivity sections, 1 m VES spacings were used. These measurements were then used to locate the position of the pipeline and the underlying subsurface geology (Dondurur 1999; Dondurur & Sarı 2003).

The subsurface geology is unconsolidated gravel deposited by a nearby stream. The apparent resistivity values for this gravel range between 40–80 ohm-m (Dondurur 1999). Although the area is relatively flat, the resistivity of the alluvial material is high due to the presence of more resistive magmatic rock fragments ranging in size between 3–30 cm in diameter. Apparent resistivity calculations were carried out after removing the effects of these blocks

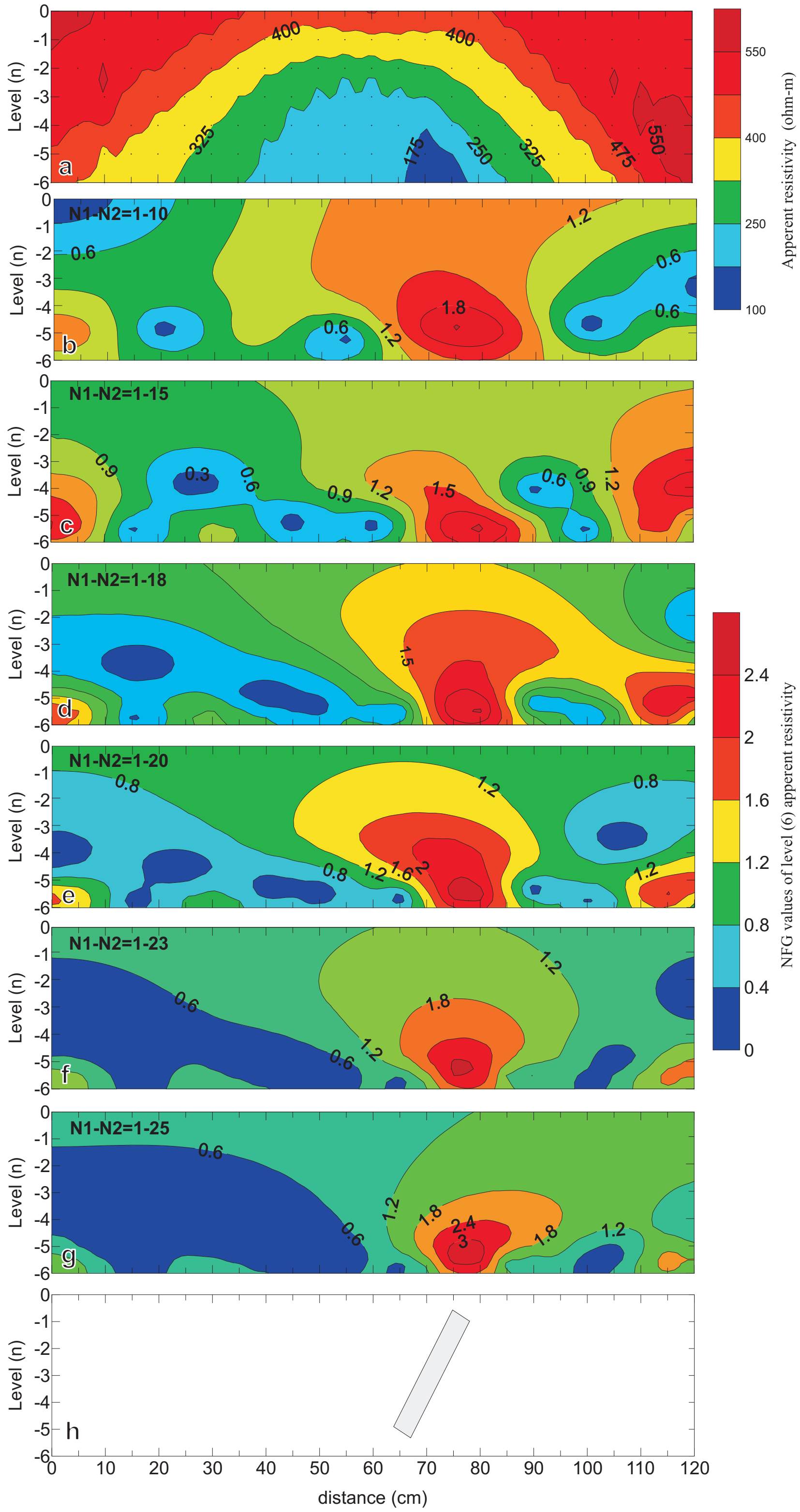

Figure 3. **(a)** Resistivity measurements on tilted dyke (Kazancı 1997), **(b–h)** NFG results, **(i)** the model.

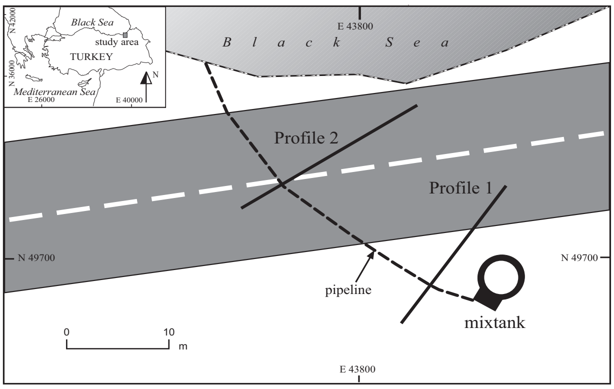

Figure 4. Highway, a buried pipe to be located, and location of four resistivity profiles taken (Dondurur & Sarı 2003).

down to 0.5 m along the profile. The resistivity sections for profiles 1 and 2 are shown in Figures 5a and 6a respectively. On both sections, the pipeline is characterized by higher apparent resistivity values than the background. The lower resistivity of the background is attributed to the possible effects of seawater, indicated because the highly conductive parts of both profiles are nearest the sea coast. It was confirmed during the construction of the road and bridge that the ground in these parts of the profiles was saturated by saline seawater. The position of the pipeline is shown as a circle on the resistivity sections (Figures 5a & 6a).

The apparent resistivity sections at the eighth electrode offset obtained in these studies was used as the input data to construct the NFG sections (values at all depths). The various NFG sections are computed using different wave-number ranges during the calculations. Measured apparent resistivity sections (Figures 5a & 6a) and the NFG sections derived from them are very similar for these profiles (Figures 5b–g & 6b–g). The NFG sections obtained for the different wave-numbers clearly show anomalous apparent resistivity values coincident with the position of the pipeline, as observed in the apparent resistivity sections (Figures 5a & 6a). The closures of the apparent resistivity values occur over the position of the pipeline. Because the discharged pipeline material is the highest apparent resistivity, both profiles show the anomaly at the same location along every profile. Besides the $[N_1,N_2]= [1,10]$ wave-number range, all the NFG sections obtained for the profiles show similar anomaly positions (both depth and lateral) for the pipeline in the apparent resistivity sections.

The pipeline anomaly is very evident on the sections obtained by two methods. Similar relationships could be made with respect to depth and location. The high apparent resistivity enclosure observed at the part of x= 8–10 m on Profile 1 was interpreted as being caused by magmatic rock blocks near the surface (Dondurur & Sarı 2003). Besides these small apparent resistivity enclosures, low apparent resistivity distributions were observed on all sections due to the effects of seawater, and since these show similar medium characteristics to those in tests in the experimental tanks, the application of the NFG method seems credible. The apparent resistivity values were rather low at Profile 2, which is very close to the sea, due to the effect of seawater. If the locations of the pipeline, which were determined from the measured and calculated NFG sections, are connected, the route can be obtained (Figure 4). This route is different from that suggested by Dondurur & Sarı (2003).

The pipeline route, drawn based on the underground sections from the apparent resistivity and NFG values, is at about n= 6–7 electrode offset depths and on x= 3.5 m at Profile 1 and x= 4.5 m at Profile 2. The extension of the profile, starting from the mixing tank to the sea, should continue as in Figure 4, according to the results of these studies.

Site #2

Another apparent resistivity profile was taken from the survey carried out in the District of Güzelyalı, in the town of Gürbulak, about 7 km south of Trabzon (NE Turkey) along the coast (Figure 7). The purpose of that survey was to determine the effects of topography on the apparent resistivity sections through modelling. Apparent resistivity calculations were acquired along a profile sloping at 10–25^o over a SE–NW-trending landslide. The fault plane of the landslide varies between 1.5–3 m. The rocks of the observed geological units of the survey area were weathered, due to climatic conditions, surface and underground waters. Increased porosity rates resulting from increased water movements reduced rock stability, and hence the slope stability was lost,

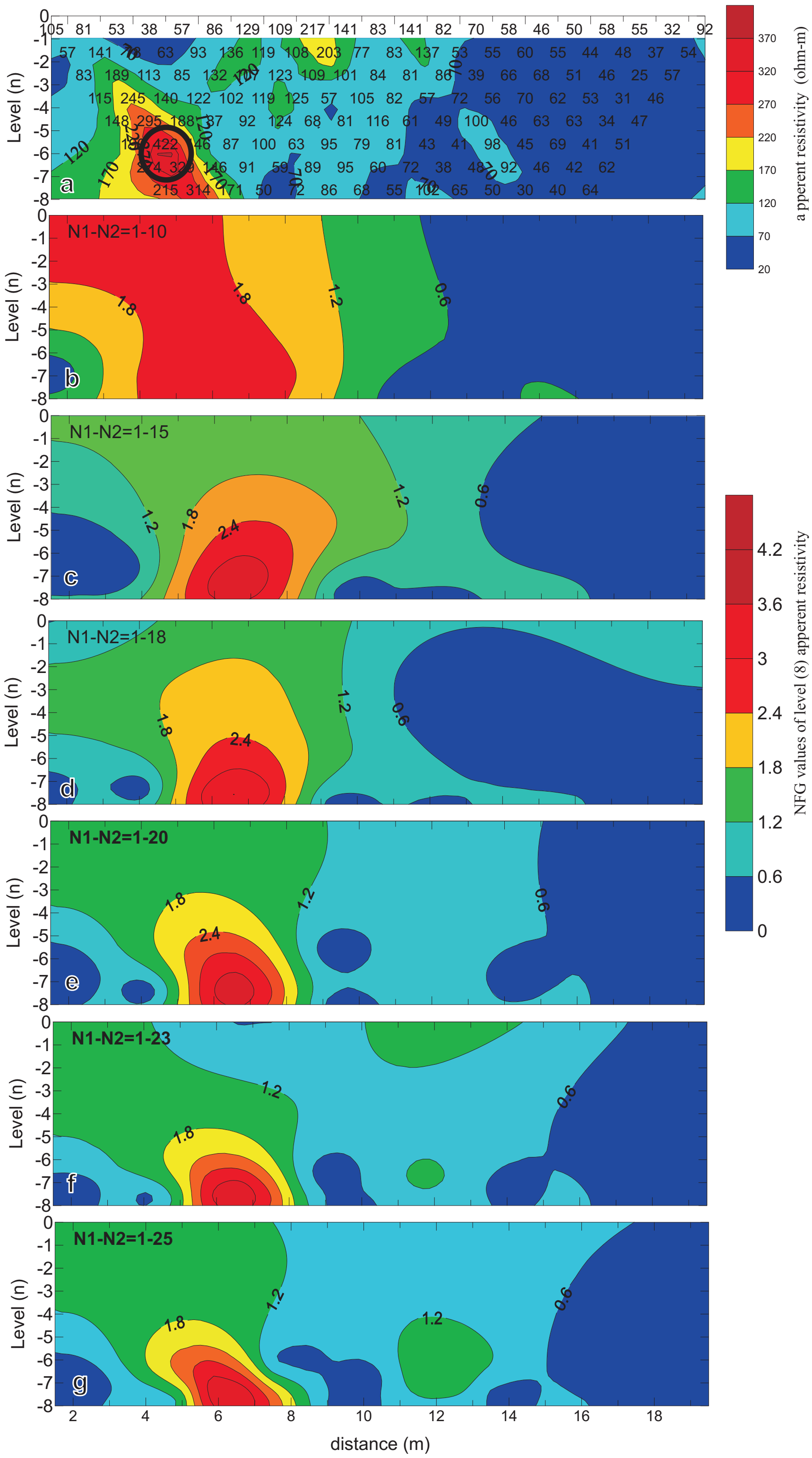

Figure 5. Profile no. 1 **(a)** resistivity measurements, **(b–g)** NFG sections obtained using different wave-number ranges.

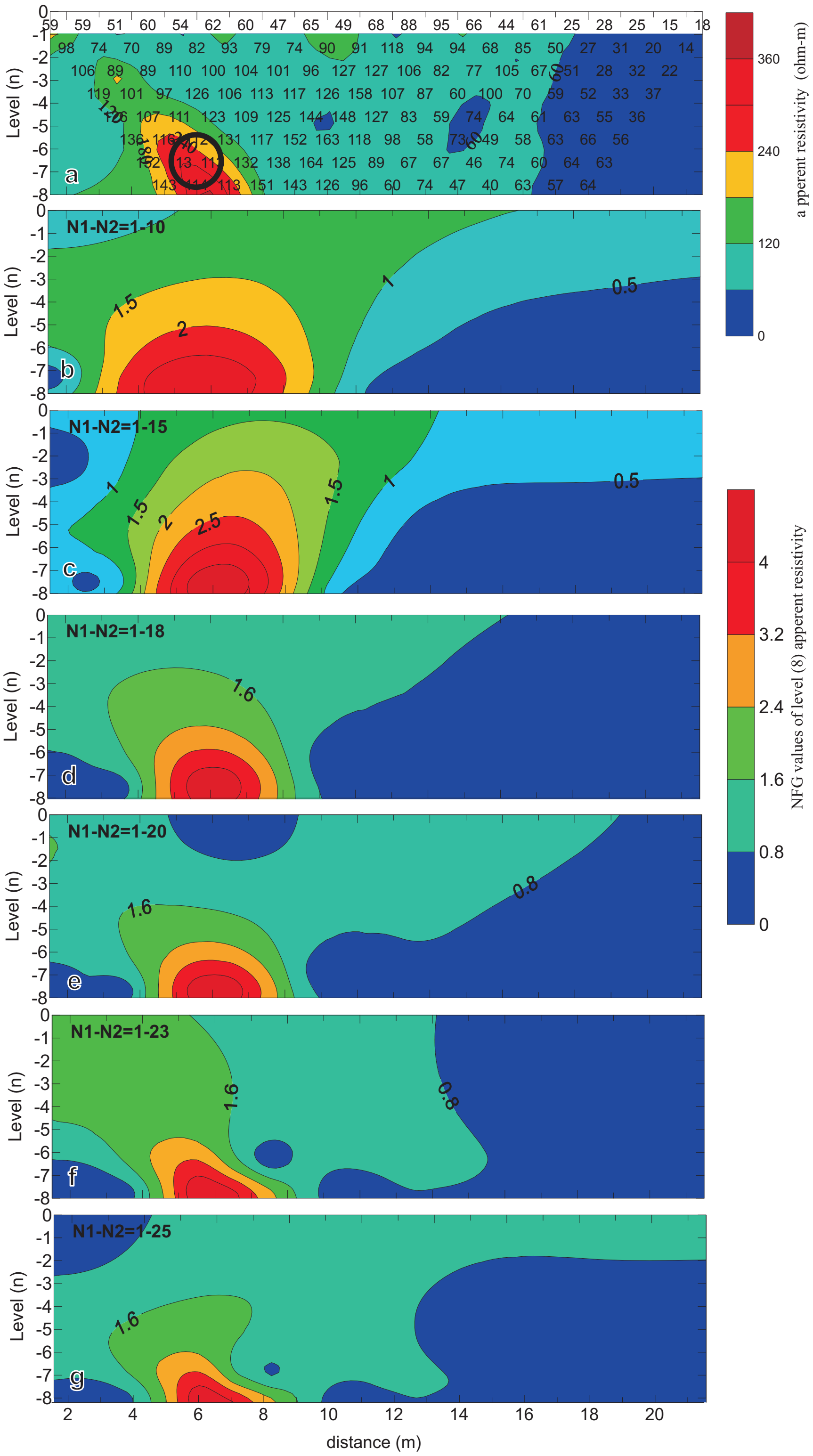

Figure 6. Profile no. 2 **(a)** resistivity measurements, **(b–g)** NFG sections obtained using different wave-number ranges.

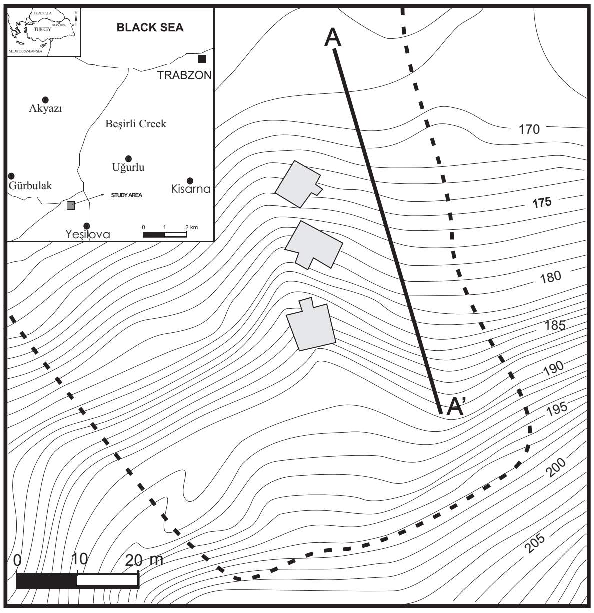

Figure 7. Location map of the second survey area (Yılmaz 2007). Dashed line shows the boundaries of the landslide and the stippled ornaments at the landslide centre show buildings.

causing a landslide. The Çağlayan, Bakırköy and Kabaköy formations were observed from geological studies in the area of the chosen profiles (Güven 1993). Outcropping marls of the landslide area, surrounded by a succession of limestones, marls, claystones and tuffites, belong to the Bakırköy formation: the marls and tuffites were reported to be at the lower electrode offsets (Yılmaz 2005). The top unit, comprising limestones and marls, is about 30 m thick. In order to investigate the landslide, profiles were made across and parallel to the slope, although only the cross profiles (NNW–SSE) were used to obtain the NFG sections in this study. The profile length is 100 m and the electrode spacing was 5 m in the electrode array. Measurements were made using the ABEM Terrameter SAS 1000 resistivity equipment (Yılmaz 2007).

Yılmaz (2005) interpreted this 2D dipole-dipole resistivity profile taken across the landslide area of the Güzelyalı District (Gürbulak, Trabzon, NE Turkey). Using the measured data, the apparent resistivity contour map of the data and the NFG sections obtained from the data at the eighth electrode offset are shown in Figure 8. Since the NW–SE profiles were along the slope, Yılmaz (2007) interpreted them after normalizing the topographic effects, so that all the data could be assumed to be taken as if on a horizontal surface. Low apparent resistivity (below 26–28 ohm-m) anomalies were observed at about 2.5–7.5 m in the model, and high apparent resistivity (above 31–34 ohm-m) anomalies were observed at depths of 12.5 m. The weathered zone is about 5 m thick and saturated with water (Yılmaz 2007). The geological section is shown in Figure 8h.

NFG sections calculated from various wave-numbers using the lowest electrode offset apparent resistivity values are shown in Figure 8b. A low resistivity anomaly was observed in between two high resistivity anomalies. The NFG section for the $[N_1,N_2]= [1,10]$ wave-number index range shows a minimum in between two maxima, similar to the apparent resistivity section. These closures were also observed for sections from $[N_1,N_2]= [1,15]$, $[N_1,N_2]= [1,30]$ and $[N_1, N_2]= [1,35]$. Only at $[N_1,N_2]= [1,20]$ were these closures of the NFG section not seen effectively, as in the other NFG sections.

Discussion and Concluding Remarks

In this study, the NFG method, which has provided successful results in the interpretation of gravity, magnetic data, and SP data, is for the first time applied to electrical apparent resistivity data in order to detect the locations of subsurface structures. The performance and reliability of the NFG method were tested on laboratory and field data from two sites. The results show that the NFG method is able to identify structures properly and the location of anomalous structures is comparable to those observed in the apparent resistivity sections. For example, the profiles 1 and 2 in the first field cross the pipeline from the southwest end. This is well observed at distances between 6 and 8th metres in Figures 5 and 6.

Also the landslide in the second field is well marked with low resistivity and in Figure 7, the buildings at the centre are in danger.

It is demonstrated here that by acquiring resistivity data at one 'n' level only, a pseudosection at

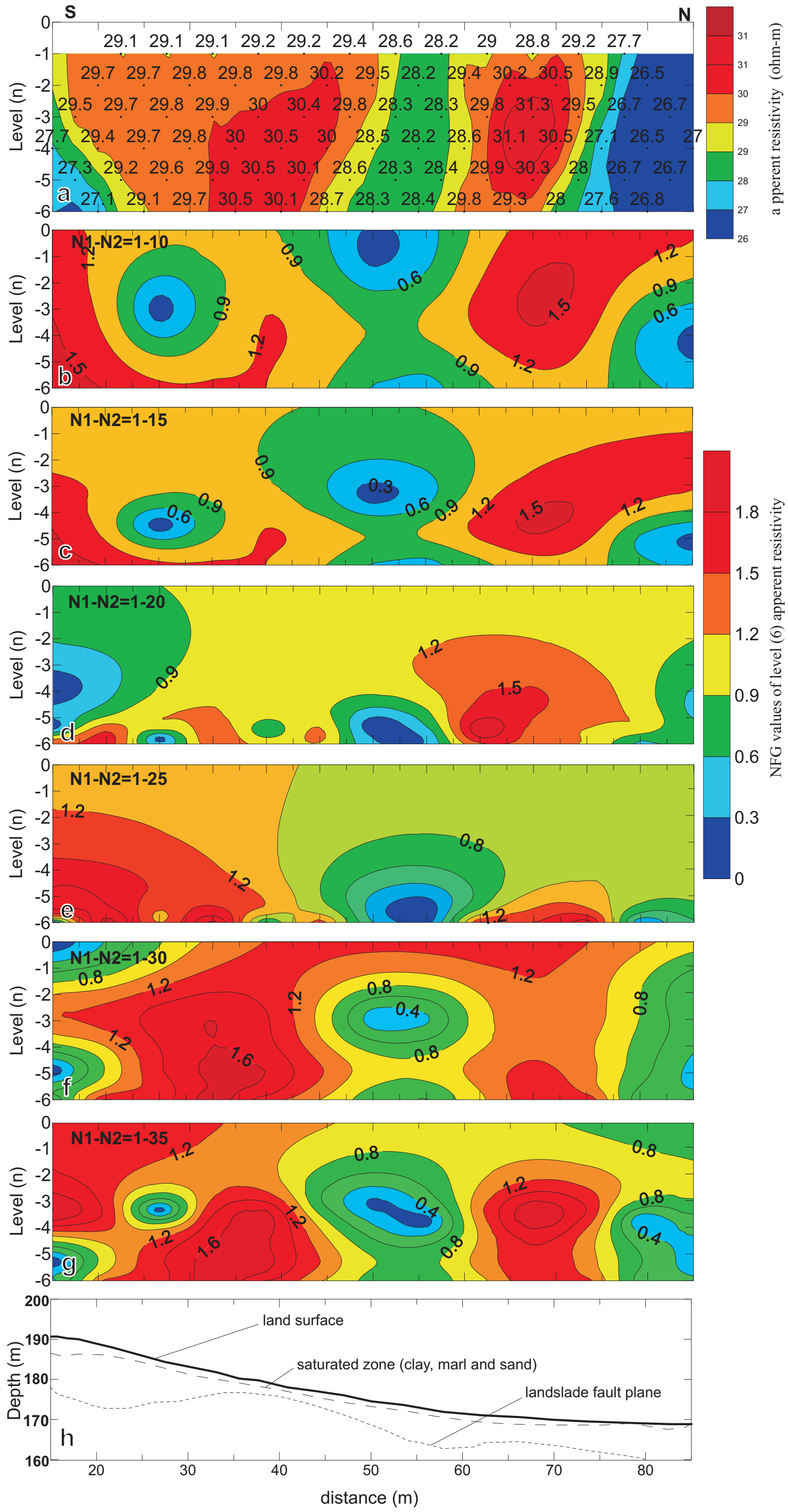

Figure 8. **(a)** Normalized resistivity data (Yılmaz 2007), **(b–h)** NFG sections obtained using 6th electrode offset's resistivity values in his figure 10 (a).

multiple depths can be calculated using the NFG technique, hence reducing the total time required to acquire data in field settings. Although it may be argued that the use of automatic switching, multiple electrode systems negates the use of NFG, in developing countries where such advanced resistivity systems are not readily available and where most resistivity acquisition still uses just four electrodes, the use of the NFG technique can provide an alternative way of acquiring resistivity data over simple targets. Thus the use of the NFG methods helps to accelerate data acquisition at multiple depths.

Acknowledgments

I would like to thank Estella A. Atekwana from Oklahoma State University, Necati Gulunay from CGG Veritas R&D, Mustafa Ergun from Dokuz Eylül University, and Abdullah Ateş from Ankara University for thoughtful reviews, many helpful suggestions in preparing the manuscript and the English language and comments. I appreciate all the help from the reviewers and editor to improve the manuscript. Also, I am very grateful to Sedat Yılmaz for allowing me the use of his field data, to Kenan Gelişli and Hakan Karslı from Karadeniz Technical University and Derman Dondurur from Dokuz Eylül University for collecting the data and helping with the survey.

References

AYDIN, A. 1997. *Evaluation of Gravity Data in Terms of Hydrocarbon by Normalized Full Gradient, Variation and Statistic Methods, Model Studies and Application in Hasankale-Horasan Basin (Erzurum).* PhD Thesis, Karadeniz Technical University, Trabzon, Turkey [unpublished].

AYDIN, A. 2000. Evaluating gravity and magnetic data by normalized full gradient. *Azerbaijan International Geophysical Conference Book, Baku*, p. 223.

AYDIN, A. 2007. Interpretation of gravity anomalies with the normalized full gradient (NFG) method and an example. *Pure and Applied Geophysics* **164**, 2329–2344.

AYDIN, A., SİPAHİ, F., KARSLI, H., GELİŞLİ, K. & KADIROV, F. 1997. Interpretation of magnetic anomalies on covered fields using normalized full gradient method. *International Geoscience Conference and Exhibition Book, Moscow*, D3., 4 p.

AYDIN, A., KADIROV, A. & KADIROV, F. 2002. Interpretation of anomalies gravity-magnetic fields and seismicity of Eastern Turkey. *'Assessment of Seismic Hazard and Risk in the Oil-Gas Bearing Areas' (100-anniversary of Shamakha Earthquake) International Conference Book*, *Baku,* p. 125.

BEREZKIN, V.M. 1973. *Method of Total Normalized Gradient*. Nedra, Moscow.

BEREZKIN, V.M. 1988. *Total Gradient Method in Geophysical Exploration.* Nedra, Moscow.

BEREZKIN, V.M. & BUKETOV, A.P. 1965. Application of the harmonic analysis for the interpretation of gravity data. *Applied Geophysics* **46**, 161–166.

BEREZKIN, V.M. & FILATOV, V.G. 1992. *The Method and the Technology for A real Processing of Gravi-magnetic Data*. Neftegeofizika, Moscow.

BRACEWELL, R. 1984. *The Fourier Transform and Its Applications*. McGraw-Hill Book Co., New York.

DAVIS, P.J. & RABINOWITZ, P. 1989. *Methods of Numerical Integration*. Academic Press, New York.

DONDURUR, D. 1999. Resistivity investigation of metal tailing discharge pipeline in Çayeli-Rize (Turkey). *2nd Balkan Geophysical Congress and Exhibition, İstanbul, Abstracts*, p. 33.

DONDURUR, D. 2005. Depth estimates for slingram electromagnetic anomalies from dipping sheet-like bodies by the normalized full gradient method. *Pure and Applied Geophysics* **161**, 2179–2196.

DONDURUR, D. & SARI, C. 2003. Investigation of buried metal waste tailing discharge pipeline by resistivity method. *Geophysics Symposium of Süleyman Demirel University, İsparta, Abstracts*, p. 41.

EBRAHIMZADEH, A.V. 2004. Detection of near-surface anomalies through 2-D normalized full gradient of gravity data. *Journal of Earth Space Physics* **30**, 1–6.

ELISEEVA, I.S., SEIBERL, W., SLAPANSKY, P., PAŠTEKA, R. & ARNDT, R. 2002. Quantitative interpretation of gravity data in the Vienna Basin region by means of the QSP-method. *In: Proceedings of the XVII. Congress of CBGA. Geologica Carpathica* **53**, 75–82.

FILON, L.N.G. 1928. On a quadrate method for trigonometric integrals. *Proceedings of Royal Society of Edinburg* **49**, 38–47.

GOLIZDRA, G.Y. 1962. On relationship between singular points of gravity potential and form anomalous masses. *2nd Conference of Young Geologist of Ukraine, Proceding*, Kiev.

GÜVEN, I.H. 1993. *1/25000 Scale Geology Map of Eastern Pontides*. Mineral Research and Exploration Institute of Turkey (MTA) Publication.

JUNG, K. 1961. Schwerkraftverfahren in der Angewandten Geophysik. *Akademische Verlagsgesellschaft Gees und Portig KG*, Leipzig, 94–95.

Karsli, H. 2001. *The Usage of Normalized Full Gradient Method in Seismic Data Analysis and a Comparison to Complex Envelope Curves*. PhD Thesis, Karadeniz Technical University, Trabzon, Turkey [unpublished].

Kazanci, F. 1997. *The Modeling of Conductive and Resistive Dikes Using the Analogue Experiment Tank and the Finite Element Method*. MSc Thesis, Karadeniz Technical University, Trabzon, Turkey [unpublished].

Lyatsky, H.V., Thurston, J.B., Brown, R.J. & Lyatsky, V.B. 1992. Hydrocarbon exploration applications of potential field horizontal gradient vector Maps. *Canadian Society of Exploration Geophysicists Recorder* **17**, 10–15.

Mudretsova, E.A., Varlamov, A.S., Filatov, V.G. & Komarova, G.M. 1979. *The Interpretation of Detailed Gravity Data Over the Nonstructural Oil and Gas Reservoirs.* Nedra, Moscow.

Nabighian, M.N. 1974. Additional comments on the analytic signal of two-dimensional magnetic bodies with polygonal cross-section. *Geophysics* **9**, 85–92.

Pašteka, R. 2000. 2D semi-automated interpretation methods in gravimetry and magnetometry. *Acta Geologica Universitatis Comeniana* **55**, 5–50.

Rikitake, T., Sato, R. & Hagiwara, Y. 1976. *Applied Mathematics for Earth Scientists.* Terra Scientific Publishing Co., Tokyo.

Sindirgi, P., Pamukcu, O. & Özyalin, S. 2008. Application of normalized full gradient method to self potential (SP) data. *Pure and Applied Geophysics* **165**, 409–427.

Strakhov, V.N. 1962. On methods of mathematical theory construction in interpretation of magnetic and gravity anomalies. *Applied Geophysics* **25**, 125–133.

Strakhov, V.N., Grİgoreva, O.M. & Lapİna, M.I. 1977. Determination of singular points of two dimensional potential fields. *Prikladnaya Geofizika* **85**, 96–113.

Traynin, P.N. & Zhdanov, M.S. 1995. Total normalized gradient method in the interpretation of airborne electromagnetic and magnetic data. *SEG Technical Program Expanded Abstracts* **14**, 232–234.

Yilmaz, S. 2005. *Two-Dimensional Finite Element Modeling and Inversion of The Dipole-Dipole Resistivity Data Including The Effect of Topography*. PhD Thesis, Karadeniz Technical University, Trabzon, Turkey [unpublished].

Yilmaz, S. 2007. Investigation of Gürbulak landslide using 2D electrical resistivity image profiling method (Trabzon, Northeastern Turkey). *Journal of Environmental* & *Engineering Geophysics* **12**, 199–205.